



# Reduced polysulfide shuttle in lithium–sulfur batteries using Nafion-based separators



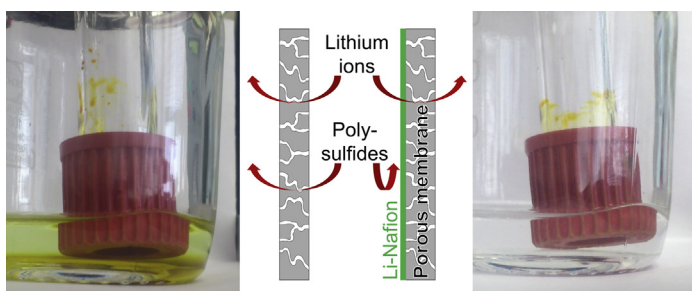
I. Bauer, S. Thieme, J. Brückner, H. Althues\*, S. Kaskel

Fraunhofer Institute for Material and Beam Technology (IWS), Winterbergstraße 28, D-01277 Dresden, Germany

## HIGHLIGHTS

- Nafion-coated propylene separator (Celgard 2500) for improved charge efficiency.
- Single-sided dense Nafion-coating after lithiation.
- Enhanced rate capability and voltage compared to free standing Nafion membranes.
- Substantial reduced polysulfide diffusion through separator.

## GRAPHICAL ABSTRACT



## ARTICLE INFO

### Article history:

Received 7 August 2013

Received in revised form

13 November 2013

Accepted 27 November 2013

Available online 7 December 2013

### Keywords:

Lithium–sulfur battery  
Lithiated Nafion-coating  
Polysulfide inhibition  
Charge efficiency  
Coated separator

## ABSTRACT

Nafion-coated polypropylene separator (Celgard 2500) is used as cation-selective membrane for lithium sulfur batteries to suppress polysulfide diffusion enhancing the charge efficiency of the cells especially at low charge/discharge rates. The charge efficiency of the 10th cycle rises from about 70% to nearly 90% at a rate of C/20. The reduction of polysulfide penetration through the Nafion-coated Celgard 2500 is also proven by visual characterization. FTIR and SEM investigations verify a smooth and dense Nafion-coating on the porous polypropylene backbone of the separator. The influence of Nafion-loading on rate capability and discharge voltage is investigated by galvanostatic charge–discharge measurements. With the lowest Nafion-loading of  $0.25 \text{ mg cm}^{-2}$  we are able to achieve a rate capability comparable to uncoated Celgard 2500 up to current densities of  $3 \text{ mA cm}^{-2}$ , whereas the functionality as polysulfide shuttle inhibitor is largely preserved.

© 2013 Elsevier B.V. All rights reserved.

## 1. Introduction

The demand for high energy batteries is increasing continuously due to wide-range application in smartphones, laptops as well as the upcoming field of electric mobility. Lithium–sulfur batteries have the potential to enhance the cell energy density in comparison to state of the art lithium-ion technology, since sulfur has a theoretical capacity of  $1672 \text{ mAh g}^{-1}$  being about eight times higher

compared to commercial cathode active materials with maximum of  $200 \text{ mAh g}^{-1}$  for nickel cobalt aluminum (NCA) materials [1,2].

In spite of the high theoretical capacity there are some serious drawbacks to overcome. One of these is the limited cycle stability of lithium–sulfur cells, caused by irreversible processes leading to continuous loss of capacity. Particularly the reduction of long chained lithium polysulfides on the lithium surface and the subsequent re-oxidation at the cathode, referred to as polysulfide shuttle mechanism, leads to parasitic self-discharge and reduced charge efficiency [3]. Furthermore, the shuttle does trigger the formation of insoluble, insulating short chained lithium polysulfide precipitates on both cathode and anode surface [4,5].

\* Corresponding author. Tel.: +49 351833913476.

E-mail address: [holger.althues@iws.fraunhofer.de](mailto:holger.althues@iws.fraunhofer.de) (H. Althues).

Different attempts have been investigated to encapsulate polysulfides in the cathode. Porous carbons with defined pore sizes and geometries providing an electrically conductive framework for sulfur have been reported to suppress polysulfide dissolution in the electrolyte and thus movement to the anode [1,6].

Another promising approach is to protect the lithium surface from reaction with polysulfides by a protective coating layer (*ex situ*) [7] or *in situ* formation of a stable solid electrolyte interface (SEI) layer by application of  $\text{LiNO}_3$  electrolyte additive [8,9]. Unfortunately  $\text{LiNO}_3$  is consumed during SEI formation on clean lithium and therefore has no enduring effect on charge efficiency due to formation of lithium dendrites upon cycling. It is also reported  $\text{LiNO}_3$  decomposes in lithium sulfur cells at voltages below 1.6 V vs.  $\text{Li/Li}^+$  [10].

Moreover it is possible to transform the separator into an ion-selective barrier being impermeable for polysulfides but permeable for lithium ions to suppress the shuttle mechanism. In this case highly accessible cathode structures like vertical aligned carbon nanotubes (VA-CNT) would take more benefit [11]. Nafion, a commercial product utilized as cation selective material in chloralkali process and fuel cells [12], is an excellent candidate to fulfill this criterion. The block-copolymer, originally developed by the E. I. DuPont Company, consists of a tetrafluoroethylene polymer backbone with sulfonic functionalized perfluorovinyl ether side chains [13]. As shown by Jin et al. lithiated Nafion membranes with thickness of 50  $\mu\text{m}$  are – in principle – capable of suppressing the shuttle when used as separators in lithium–sulfur batteries [14]. Although their cells were cycled at a low current density of  $0.3 \text{ mA cm}^{-2}$  the voltage (vs.  $\text{Li/Li}^+$ ) of the second discharge plateau was largely reduced from 2.1 V to 1.9 V, evidencing a high ion transport resistance induced by the Nafion membrane thickness. Thinner membranes may reduce the voltage drop; however, no free standing membranes with a thickness of less than 25  $\mu\text{m}$  are commercially available due to limited mechanical integrity. For fuel cell applications a Nafion-coating of porous polypropylene separator (Celgard 2500) was reported to overcome this drawback [15]. We utilize a lithiated thin Nafion film applied on a Celgard 2500 as support structure enabling high current densities and suppressing the polysulfide shuttle.

Very recently Tang et al. reported of a Nafion coated sulfur–carbon cathode improving the charge efficiency and capacity of lithium sulfur cells [16]. However, the applied coating has a thickness of about 10  $\mu\text{m}$  and no statements about current densities were made.

In this paper we investigate the suitability of a thin polysulfide blocking film (Nafion, thickness about 1–5  $\mu\text{m}$ ) on porous polypropylene backbone (Celgard 2500) for application in lithium–sulfur batteries. The lithiated form of Nafion was utilized and the influence of its areal loading was tested in terms of charge efficiency as well as rate capability in the liquid electrolyte lithium sulfur cell.

## 2. Experimental

The coating of Celgard 2500 with Nafion (referred as H–Nafion@Celgard) was performed by a drop-coating procedure. Nafion dispersion (Nafion dispersion D2020, 20 wt% in alcohol/water base, Ion Power) was diluted to 1.25, 2.5 or 5 wt% by addition of ethanol (99.8%, Carl Roth) depending on the desired Nafion-loading of 0.25, 0.5 or  $1.0 \text{ mg cm}^{-2}$  and subsequently dropped on the Celgard 2500 backbone. Thereby, special attention was paid to the homogenous distribution of the wet film, which brought up the necessity of using solutions with different Nafion-concentrations to not only adjust the loadings but also achieve a dense and smooth coating. The coated membranes were dried at room temperature overnight and subsequently for 1 h at 55  $^{\circ}\text{C}$  in air. The lithiation process was carried out in aqueous 1 M  $\text{LiOH}$  solution at 80  $^{\circ}\text{C}$  for 14 h. To remove salt, the coated and lithiated separator was treated at 80  $^{\circ}\text{C}$  for 1 h in water. The resulting separators are referred as Li–Nafion@Celgard. Previous to cell assembly the separator sheets were dried at 80  $^{\circ}\text{C}$  for 30 min.

The cathodes were prepared by mixing sulfur (Sigma Aldrich,  $\geq 99.5\%$ ), conductive carbon (Timcal Super C65) and multiwall carbon nanotubes (MWCNT, Nanocyl NC7000) and mild grinding in a mortar mill (Fritsch Pulverisette 2) for 10 min. Subsequently a water based binder solution of carboxy methyl cellulose (CMC, MTI Corporation) & styrene-butadiene rubber (SBR, Targray) (ratio CMC:SBR = 1:1, m:m) was added and the slurry was treated for 30 min in the mortar grinder again. The weight ratio of sulfur:SuperC65:MWCNT:CMC:SBR in the resulting slurry was 45:45:5:2.5:2.5. The slurry was casted onto carbon coated (Electrodag EB-012) aluminum foil (MTI Corporation,  $>99.9\%$ ) via doctor-blade coating technique. Drying of the as-prepared cathode sheets consisted of two steps, drying over night at room temperature and afterward at 80  $^{\circ}\text{C}$  for 1.5 h. The thickness of the dry active layer was determined to be approx. 60  $\mu\text{m}$  corresponding to a sulfur loading of about  $1.6 \text{ mg cm}^{-2}$ .

The electrochemical measurements were performed in 2016 coin cells (MTI Corporation) using cathodes of 12 mm diameter. Metallic lithium chips (Pi-Kem, 99.0%) with 15.6 mm diameter and 250  $\mu\text{m}$  thickness were used as anode. The electrolyte consisted of 1 M lithium bis(trifluoromethylsulfonyl)imide (LiTFSI, Aldrich, 99.95%) dissolved in a 1:1 (v:v) mixture of 1,2-dimethoxy ethane (DME, Sigma Aldrich, 99.5%, anhydrous) and 1,3-dioxolane (DOL, Sigma Aldrich, 99.8%, anhydrous). To ensure a tight separation between anode and cathode space, the separator (19 mm diameter) was pressed between the bottom of the stainless steel case and the seal of the cell connected to the upper part of the stainless steel case (Fig. 1a). Consequently, the electrolyte cannot migrate between anode and cathode space by evading the separator through bypassing it. All cells were assembled in an argon-filled glove box with  $\text{O}_2$  and  $\text{H}_2\text{O}$  content below 0.1 ppm.

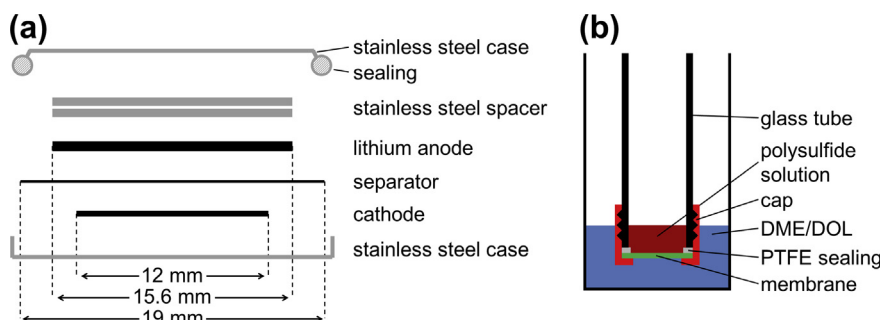


Fig. 1. (a) Schematic side view of a modified coin cell showing the separation of anode and cathode room. (b) Test setup for polysulfide diffusion experiments.

Cycling tests were performed on a BaSyTec CTS system. A test scheme with sequential current rates of C/20, C/10, C/5, C/2 and 1C (1C equals  $1672 \text{ mA g}^{-1}(\text{S})$ ) was used. Cells with plain Celgard 2500 were discharged to a voltage (vs.  $\text{Li}/\text{Li}^+$ ) of 1.8 V and recharged to 2.6 V for rates of C/20, C/10, C/5, whereas discharge and charge were terminated at 1.5 V and 2.9 V for C-rates of C/2 and 1C. Cells comprising Nafion-coated Celgard 2500 separators were discharged to 1.5 V and charged to 2.9 V for all C-rates.

In order to optically determine the retention of polysulfide species by the introduced Nafion@Celgard membrane, we used the setup shown in Fig. 1b. Thereby, 0.5 ml solution of 0.5 M  $\text{Li}_2\text{S}_6$  (nominal concentration) in DME:DOL (1:1, v:v) was placed inside the glass tube, whereas the opposite side of the separator was filled with a pristine mixture of 10 ml DME:DOL (1:1, v:v). During the experiment the solutions rested without movement to exclude external influence on the diffusion test of polysulfides through the non-modified/Nafion-modified separator. The resulting color change was evaluated by visual examination.

Attenuated total reflection (ATR) spectra were acquired with a Fourier transform infrared (FTIR) spectrometer Perkin Elmer Spectrum 2000 Golden Gate ATR for wavenumbers of  $4000\text{--}600 \text{ cm}^{-1}$ . A Zeiss DSM 982 Gemini was used for scanning electron microscopic (SEM) measurements. All samples were sputtered with gold to ensure electric conductivity.

### 3. Results and discussion

#### 3.1. Nafion-coating and lithiation of Nafion-coating on Celgard 2500

FTIR spectroscopy allows analysis of the coating of Celgard 2500 with Nafion. Fig. 2 shows the ATR spectra of untreated versus Nafion@Celgard in protonated ( $\text{H}^+$ , H–Nafion@Celgard) and lithiated ( $\text{Li}^+$ , Li–Nafion@Celgard) form. The peak around  $1710 \text{ cm}^{-1}$  corresponding to the  $\text{H}^+$  form shifts to  $1630 \text{ cm}^{-1}$  indicating the exchange of  $\text{H}^+$  with  $\text{Li}^+$  [17], which is furthermore evidenced by the disappearance of the weak peak at  $924 \text{ cm}^{-1}$ . Since peaks corresponding to Celgard 2500 almost vanish after Nafion-coating the formation of a dense film can be assumed, lithiation of the coating also does not influence the uniformity of the film. Analysis of SEM images (Fig. 3) supports these results. The pores initially existing in Celgard 2500 (Fig. 3a) are covered by a dense and homogeneous film (Fig. 3b). It may be noted that the black dot in the middle of Fig. 3b is a focal spot of the electron beam, which burned the sensitive Nafion polymer.

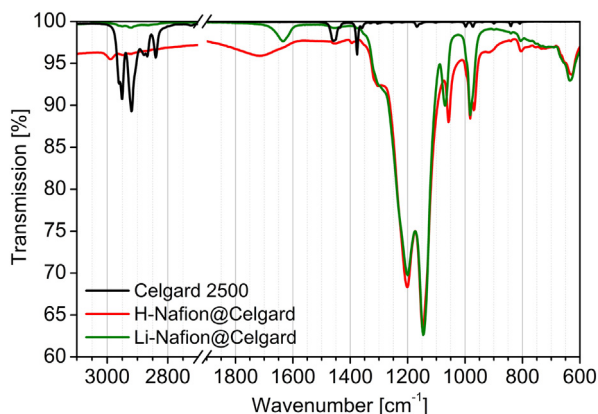


Fig. 2. ATR spectra of untreated Celgard 2500 versus Nafion-coated Celgard 2500 in  $\text{H}^+$  (H–Nafion@Celgard) and  $\text{Li}^+$  (Li–Nafion@Celgard) form. In both cases the coated side was measured.

ATR spectroscopy also was applied to determine whether there is a Nafion-coating on Celgard 2500 or Nafion is soaked through the pores of Celgard 2500. As can be seen in Fig. 4 the Nafion-coated side of Celgard 2500 shows the spectra of Nafion, implying a dense Nafion-coating (the depth of measurement is about  $1 \mu\text{m}$ ). In clear contrast, the uncoated side of Celgard 2500 shows nearly the same spectrum as Celgard 2500, except for two small peaks at around  $1200 \text{ cm}^{-1}$  which may be attributed to C–F-vibrations in Nafion [18]. This in fact proves that the coating is applied only onto one side of the Celgard 2500 separator and does not pervade the support structure.

#### 3.2. Electrochemical performance

As shown in Fig. 5 the cell voltage of the second discharge plateau cell depends on the chemical form of Nafion. While the protonated membrane (H–Nafion@Celgard) has a voltage of about 2.0 V at a rate of C/20, Li–Nafion@Celgard has a voltage of 2.1 V – comparable to the uncoated Celgard 2500. The loading branches show a similar shift of voltages. This indicates an increased ionic conductivity of lithium ions in lithiated Nafion, leading to reduced overpotential. Moreover, the cells comprising the uncoated separator do not reach the cut off voltage due to extensive shuttling at low current density. In contrast, the cells with Nafion-coated separators show a sharp voltage increase at the end of charge, thus evidencing the reduced polysulfide shuttle.

Jin et al. observed a voltage of about 1.9 V for the second discharge plateau when using a  $50 \mu\text{m}$  thick lithiated membrane of Nafion-212 at a current density of  $0.3 \text{ mA cm}^{-2}$  [14]. The equivalent measurement of Li–Nafion@Celgard has a discharge voltage of 2.1 V, which proves the enhanced ionic conductivity of the Li–Nafion@Celgard membranes (Fig. 6). The main reason for the higher voltage is the reduced resistivity of the Li–Nafion-coating compared to the free standing membranes (theoretical thickness of Li–Nafion-layer is only  $1.25 \mu\text{m}$  for a Nafion-loading of  $0.25 \text{ mg cm}^{-2}$ ). As can be seen in Fig. 7 the first plateau of cells using untreated Celgard 2500 at a rate of C/20 is not well established due to extensive polysulfide shuttling during the previous charge process and therefore not reaching the cut off voltage. This leads to a lower voltage at the beginning of discharge, because the discharge reaction starts with low chained polysulfides instead of elemental sulfur.

The rate capability of batteries is an important factor for manifold applications, as the demand of power density is highly varying especially in the field of electric mobility. Higher current densities generally lead to increased polarization and therefore not only lower discharge voltage but also capacity. In fact, it has to be taken into account that the decreasing capacity with increasing C-rate is also attributed in general to a loss of capacity with ongoing cycling (see also Fig. 8a). Especially for high current densities of  $1.5 \text{ mA cm}^{-2}$  (C/2) and  $3.0 \text{ mA cm}^{-2}$  (1C) a voltage drop in the second plateau to about 2.0 V and 1.8 V can be observed for a Li–Nafion@Celgard separator with  $0.25 \text{ mg cm}^{-2}$  Li–Nafion-loading (Fig. 6). Untreated Celgard 2500 shows a less distinct voltage drop at these currents (Fig. 7), indicating that the ionic conductivity of the modified separator is limited even in the case of a thin Li–Nafion film.

As stated earlier the Nafion-loading has a direct influence on the electrochemical performance of the cell because of the high impact on the ionic conductivity and the polysulfide retention. Two opposing factors have to be taken into account. The thinner the coated Nafion-layer (equal to lower loading), the higher is the ionic conductivity of the separator. This is due to the fact that conductivity is indirect proportional to the layer thickness, meaning that halve the layer thickness doubles the ionic bulk conductivity. On the other hand the consequent reduction of thickness of the

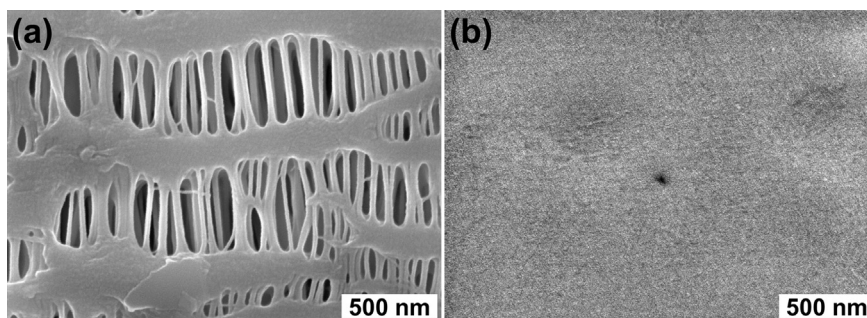


Fig. 3. SEM images of untreated Celgard 2500 (a) and H-Nafion@Celgard with  $0.5 \text{ mg cm}^{-2}$  Nafion-loading (b).

Nafion-coating increases the threat of defects in the film, being detrimental for restriction of polysulfides passing. Fig. 9 shows discharge profiles for different Li-Nafion-loadings. A higher Li-Nafion-loading leads to lower cell voltage. Whereas, a Li-Nafion-loading of  $0.25 \text{ mg cm}^{-2}$  the discharge voltage is nearly equal to untreated Celgard 2500 at 0.1C, the discharge profiles for Li-Nafion-loadings of 0.5 and  $1.0 \text{ mg cm}^{-2}$  show more sloping characteristics, suppressed voltage plateaus as well as earlier end of discharge due to the higher internal resistivity of the membrane.

Cells based on plain Celgard 2500 as well as Li-Nafion@Celgard have initial discharge capacities of about  $1100 \text{ mAh g}^{-1}(\text{S})$  at 0.05C (Fig. 8a). In the subsequent cycles, batteries with uncoated Celgard 2500 show immediate loss of capacity to approx.  $850 \text{ mAh g}^{-1}(\text{S})$  because they are not reaching the cut off voltage and therefore low charge efficiency as well as polysulfide diffusion to the anode occur. When increasing the C-rates it can be observed that lower Li-Nafion-loadings lead to better rate capability. Up to 0.2C membranes with a Li-Nafion-loading of  $0.25 \text{ mg cm}^{-2}$  exhibit 50–100  $\text{mAh g}^{-1}(\text{S})$  more capacity than pure Celgard 2500, indicating fewer losses through polysulfides. At charge/discharge rates of 0.5C and 1C the drop of capacity for Li-Nafion-coated separators ( $0.25$  &  $0.5 \text{ mg cm}^{-2}$ ) increases quite drastic in comparison to uncoated Celgard 2500 due to limitations in lithium ion conductivity through the membranes. In this regard Li-Nafion-loadings of less than  $0.25 \text{ mg cm}^{-2}$  would be desirable to achieve a better rate capability. However, with impregnation technique currently applied coating with less than  $0.25 \text{ mg cm}^{-2}$  does not form a dense film on Celgard 2500, due to inhomogeneous drying of the drop coated film. New coating techniques like spray coating or dip coating might be able to overcome this issue and therefore will be studied in future work.

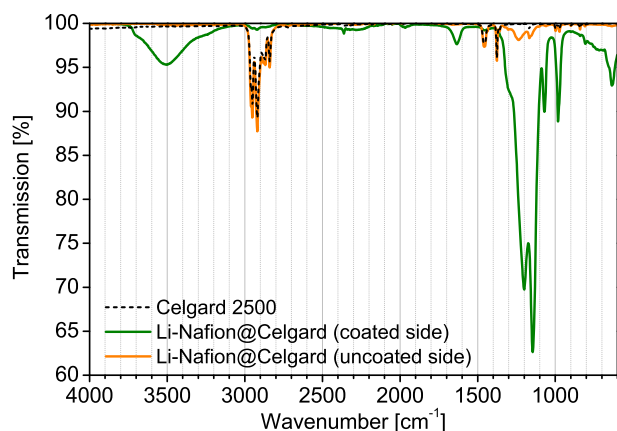


Fig. 4. ATR spectra of both sides of a Li-Nafion@Celgard separator (Li-Nafion-loading  $0.5 \text{ mg cm}^{-2}$ ). The spectrum of untreated Celgard 2500 was added for comparison.

In contrast, high Li-Nafion-loading of  $1.0 \text{ mg cm}^{-2}$  drastically reduces the rate capability. Beginning at C/5 the capacity fades quickly and at C/2 as well as 1C the cells did not deliver any capacity highlighting that insufficient overall ionic conductivity of the coated membrane limits the rate capability.

A feasible indicator for the intensity of the polysulfide shuttle mechanism is the charge efficiency. As shown in Fig. 8b Li-Nafion@Celgard separators show improved charge efficiencies (CE),

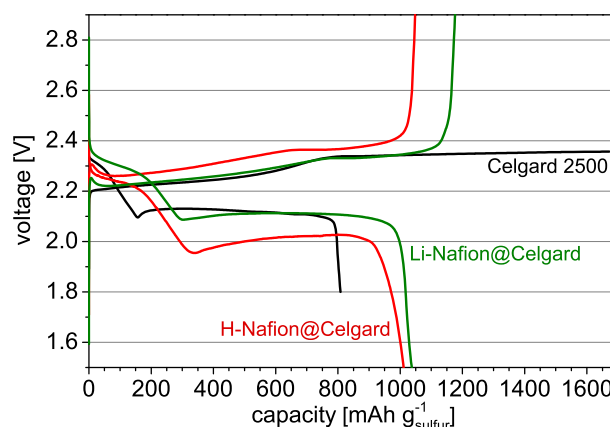


Fig. 5. Voltage profiles of the third cycle of lithium-sulfur coin cells of untreated Celgard 2500 and H- respectively Li-Nafion@Celgard (H-/Li-Nafion loading  $0.5 \text{ mg cm}^{-2}$ ). All shown cells did not contain  $\text{LiNO}_3$ . The C-rate was C/20, corresponding to a current density of approximately  $0.15 \text{ mA cm}^{-2}$ .

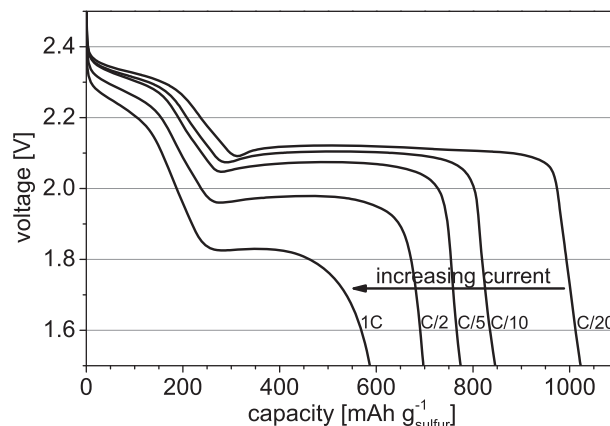
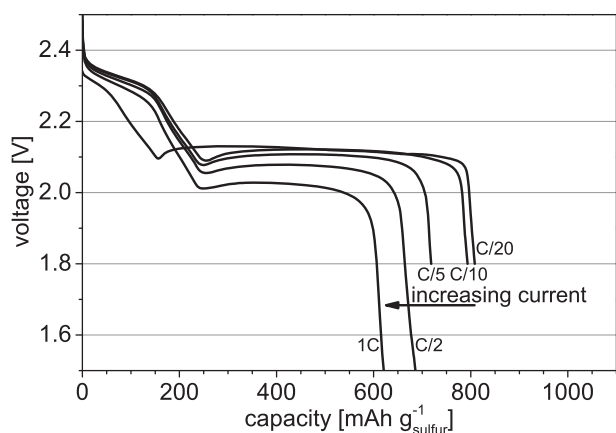


Fig. 6. Discharge voltage profiles of Li-Nafion@Celgard separator at different C-rates (1C is corresponding to about  $3 \text{ mA cm}^{-2}$ , Li-Nafion loading  $0.25 \text{ mg cm}^{-2}$ ). The shown voltage profiles represent the third cycle of each C-rate stage, meaning the 3rd (C/20), 13th (C/10), 23rd (C/5), 33rd (C/2) and 43rd (1C) overall cycle.





**Fig. 7.** Discharge voltage profiles of the untreated Celgard 2500 at different C-rates (1C is corresponding to about  $3 \text{ mA cm}^{-2}$ ). The shown voltage profiles represent the third cycle of each C-rate stage, meaning the 3rd (C/20), 13th (C/10), 23rd (C/5), 33rd (C/2) and 43rd (1C) overall cycle.

especially at low C-rates. Surprisingly Li–Nafion-loadings of 0.25 and  $0.5 \text{ mg cm}^{-2}$  possessed approximately the same positive effect, whereas increasing the loading to  $1.0 \text{ mg cm}^{-2}$  did not improve the charge efficiency but lead to failure after a few tens of cycles.

To verify the results of the charge efficiency tests the polysulfide retention of the membranes was tested with a polysulfide containing solution (Fig. 10). As was expected, the pristine polypropylene separator did not suppress the diffusion of polysulfides,

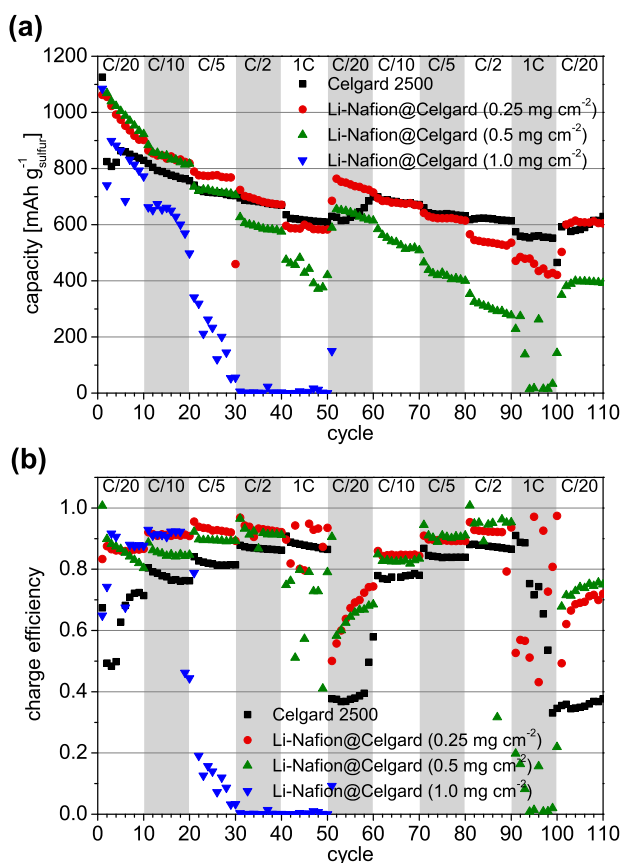


**Fig. 8.** Discharge capacities at different C-rates (a) and charge efficiencies (b) of untreated Celgard 2500 versus Li–Nafion@Celgard with Li–Nafion-loadings of 0.25, 0.5 and  $1.0 \text{ mg cm}^{-2}$ .

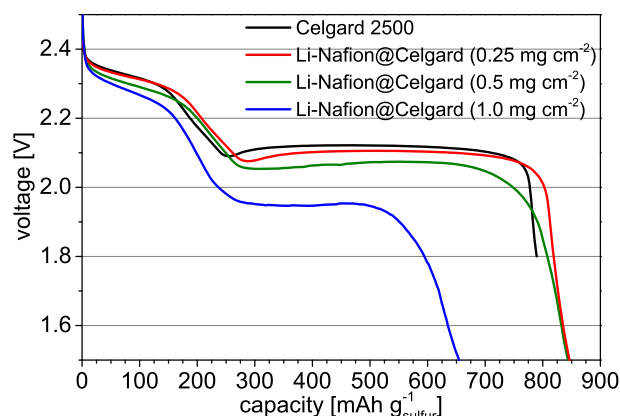


**Fig. 9.** Discharge voltage profiles of Li–Nafion@Celgard separators for different Li–Nafion-loadings versus uncoated Celgard 2500 at a C-rate of 0.1C (approx.  $0.3 \text{ mA cm}^{-2}$ ). The shown voltage profiles represent the third cycle of the 0.1 C-rate stage (13th cycle of whole measurement).

thus the color of the DME:DOL mixture already changed from colorless to green after 5 min of rest (Fig. 10a), indicating diffusion of short chained polysulfides [19]. After 90 min elapsed a brown reddish solution was obtained due to diffusion of long chained polysulfides from the reservoir through the separator, whose color remained stable for another 150 min (Fig. 10b and c). In contrast, H–Nafion@Celgard (H–Nafion-loading  $0.5 \text{ mg cm}^{-2}$ ) largely suppressed the diffusion of polysulfide species. Therefore even after 4 h of rest only a slightly green coloring of the solution was observed. However, the diffusion of short chained polysulfides was not prevented perfectly, which might be attributed to their small size enabling the diffusion through the negatively charged membrane ( $\text{SO}_3^-$  groups), although rejection was expected due to repulsive interaction with negatively charged polysulfides.

This diffusion experiment may also give an explanation for the relatively low charge/discharge efficiencies of the Li–Nafion@Celgard membranes at the second and third C/20 steps in contrast to the first C/20 cycles (Fig. 8b). During cycling at higher current densities the polysulfide shuttle is not well established, therefore the concentration of polysulfides in the anode space increases due to the slow, but present diffusion of polysulfides through the Li–Nafion@Celgard separator. If applying small current densities again, these polysulfides are consumed while participating the polysulfide shuttle. After depletion of polysulfides in the anode space the charge/discharge efficiency increases for the following cycles because of the hindered transport of polysulfides through the Li–Nafion@Celgard membrane.

#### 4. Conclusions

In this paper, we showed that Nafion can be homogeneously casted onto to a Celgard 2500 support structure by a simple drop coating procedure to obtain different Nafion-loadings. The formation of a dense Nafion film was proven by SEM and ATR investigations. The lowest of  $0.25 \text{ mg cm}^{-2}$  of lithiated Nafion on the separator led to both, good rate capability and enhanced charge efficiency of the Li–S cells, whereas the influence on the discharge voltage was negligible. This is an obvious enhancement compared to free standing, lithiated Nafion membranes, which cause a voltage drop of about 0.2 V even at a modest current density of  $0.3 \text{ mA cm}^{-2}$  [14].

At low current densities cells comprising Li–Nafion@Celgard can achieve higher as well as more stable capacities than untreated Celgard 2500 due to the polysulfide shuttle is effectively suppressed. However, high Li–Nafion-loadings of 0.5 and  $1.0 \text{ mg cm}^{-2}$

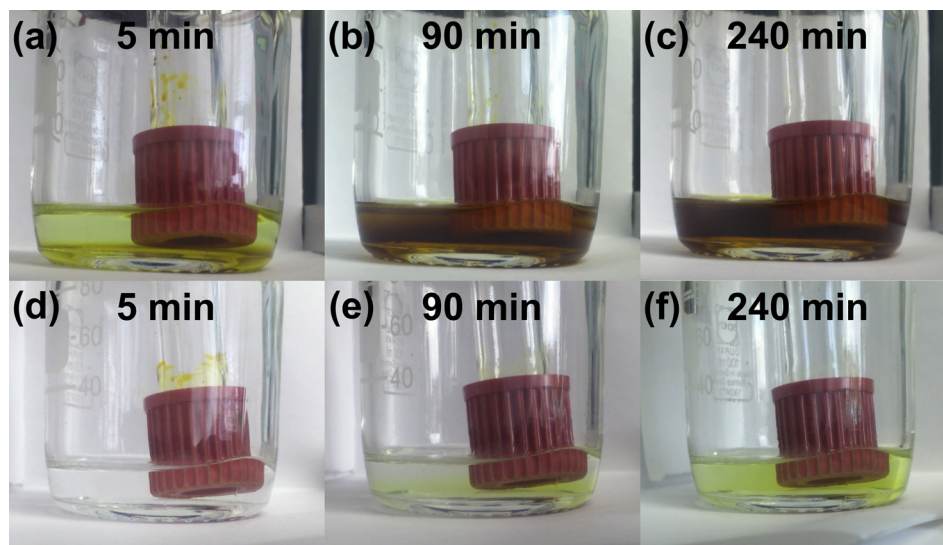


**Fig. 10.** Polysulfide diffusion test of untreated Celgard 2500 (a–c) and H–Nafion@Celgard with  $0.5 \text{ mg cm}^{-2}$  H–Nafion-loading (d–f) after variable resting times.

did not improve the charge efficiency compared to  $0.25 \text{ mg cm}^{-2}$ . In contrast, these loadings led to strongly increased polarization and failure of the cells after fewer cycles.

## References

- [1] X. Ji, L. Nazar, *J. Mater. Chem.* 20 (2010) 9821–9826.
- [2] M.M. Doeff, in: R.A. Meyers (Ed.), *Encyclopedia of Sustainability Science and Technology*, Springer, New York, NY, 2012, pp. 5–49.
- [3] Y.V. Mikhaylik, J.R. Akridge, *J. Electrochem. Soc.* 151 (2004) A1969–A1976.
- [4] E. Peled, Y. Sternberg, *J. Electrochem. Soc.* 136 (1989) 2–6.
- [5] J. Akridge, *Solid State Ionics* 175 (2004) 243–245.
- [6] S. Thieme, J. Brückner, I. Bauer, M. Oschatz, L. Borchardt, H. Althues, S. Kaskel, *J. Mater. Chem. A* (2013) 9225–9234.
- [7] Y.M. Lee, N.-S. Choi, J.H. Park, J.-K. Park, *J. Power Sources* 119–121 (2003) 964–972.
- [8] D. Aurbach, E. Pollak, R. Elazari, *J. Electrochem. Soc.* 156 (2009) A694–A702.
- [9] Y.V. Mikhaylik, *Electrolytes for Lithium Sulfur Cells*, U.S. Patent 7354680 B2, 2008.
- [10] S.S. Zhang, *Electrochim. Acta* 70 (2012) 344–348.
- [11] S. Dörfler, M. Hagen, H. Althues, J. Tübke, S. Kaskel, M.J. Hoffmann, *Chem. Commun.* 48 (2012) 4097–4099.
- [12] C. Heitner-Wirguin, *J. Membr. Sci.* 120 (1996) 1–33.
- [13] K.A. Mauritz, R.B. Moore, *Chem. Rev.* 104 (2004) 4535–4585.
- [14] Z. Jin, K. Xie, X. Hong, Z. Hu, X. Liu, *J. Power Sources* 218 (2012) 163–167.
- [15] K. Nouel, P. Fedkiw, *Electrochim. Acta* 43 (1998) 2381–2387.
- [16] Q. Tang, Z. Shan, L. Wang, X. Qin, K. Zhu, J. Tian, X. Liu, *J. Power Sources* 246 (2013) 253–259.
- [17] S. Sachan, C.A. Ray, S.A. Perusich, R. Hall, S. Sachun, *Polym. Eng. Sci.* 42 (2002) 1469–1480.
- [18] S. Perusich, *J. Appl. Polym. Sci.* 120 (2011) 165–183.
- [19] Y. Li, H. Zhan, S. Liu, K. Huang, Y. Zhou, *J. Power Sources* 195 (2010) 2945–2949.